HHS Public Access

Author manuscript

Nat Genet. Author manuscript; available in PMC 2016 June 21.

Published in final edited form as:

Nat Genet. 2012 October ; 44(10): 1104–1110. doi:10.1038/ng.2396.

Integrative genome analyses identify key somatic driver mutations of small cell lung cancer

A full list of authors and affiliations appears at the end of the article.

Abstract

Small-cell lung cancer (SCLC) is an aggressive lung tumor subtype with poor survival[1–3]. We sequenced 29 SCLC exomes, two genomes and 15 transcriptomes and found an extremely high mutation rate of 7.4±1 protein-changing mutations per million basepairs. Therefore, we conducted integrated analyses of the various data sets to identify pathogenetically relevant mutated genes. In all cases we found evidence for inactivation of *TP53* and *RB1* and identified recurrent mutations in histone-modifying genes, *CREBBP*, *EP300*, and *MLL*. Furthermore, we observed mutations in *PTEN*, in *SLIT2*, and *EPHA7*, as well as focal amplifications of the *FGFR1* tyrosine kinase gene. Finally, we detected many of the alterations found in humans in SCLC tumors from *p53/Rb1*-deficient mice[4]. Our study implicates histone modification as a major feature of SCLC, reveals potentially therapeutically tractable genome alterations, and provides a generalizable framework for identification of biologically relevant genes in the context of high mutational background.

Keywords

small-cell lung cancer; cancer genome; integrated analysis

Small-cell lung cancer (SCLC; ~15% of all lung cancer cases) typically occurs in heavy smokers and is characterized by aggressive growth, frequent metastases and early death[1,2,5]. Unfortunately, no single molecularly targeted drug has yet shown any clinical activity in SCLC6. Genomic analyses have revealed genetically altered therapeutic targets in lung adenocarcinoma[7–16] and in squamous-cell lung carcinoma[17–19]. By contrast, little is known about the molecular events causing SCLC beyond the high prevalence of mutations in *TP53* and *RB13*. Systematic genomic analyses in SCLC are challenging because these tumors are rarely treated by surgery resulting in a lack of suitable fresh-frozen tumor specimens.

Correspondence to: Roman Thomas, roman.thomas@uni-koeln.de, Department of Translational Genomics, University of Cologne, Weyertal 115b, 50931 Cologne, Germany, Tel.: +49-221-478-98771.

*These authors contributed equally to this work.

Data Access

Binary sequence alignment data of 300bp regions around all identified somatic mutations and SNP array data were deposited in the European Genome-Phenome Archive (EGA; EGAS00001000299).

Author Contributions

MP, LFC contributed equally. MP, LFC, MLS, JG, DS, LHK, FL, RM, JV, PS, JS, RS, RB, SP, LH, PKB, RKT conceived and designed the experiments. LFC, MLS, JG, DS, LHK, DP, RM, MK, ID, CM, VDC, HUS, JA, IB, CB, BDW, DB, FG, IW, SH, JH preformed experiments. MP, LFC, MLS, JG, DS, LHK, DP, FL, RS, TZ, RM, VDC, BDW, JV, XL, WP, MLW, JS, RS, SP, LH, PKB, SH, RKT analyzed the data. MP, RS, TZ, SA, SLC, KC, SB, GG, KSP, DR, CG, MF, LP, GW, ZW, PR, IP, YC, ES, CL, PS, HH, TM, MB WER, LAM, VMF, HG, WT, HS, ET, ES, DAMH, PJFS, FC, CL, SD, JF, SS, OTB, MLI, JS, JHC, AS, HM, WW, BS, JCS, BB, EB, CB, SL, MH, JS, JW, PN, LH, PKB, SH contributed reagents/materials/analysis tools. MP, LFC, RKT wrote the paper.

We have established a global lung cancer genome research consortium[19], giving us access to approximately 6,600 surgically resected lung cancer specimens, out of which we retrieved 99 SCLC specimens. We conducted 6.0 SNP array analyses on 63 tumors, exome sequencing of 27 tumors and two cell lines, transcriptome sequencing of 15 tumors, and genome sequencing of two tumors (Supplementary Tab. 1).

We applied a novel algorithm in order to identify significant broad (Supplementary Fig. 1a) and focal copy number alterations (CNAs) (Fig. 1a, Supplementary Tab. 2) and observed almost universal deletions affecting 3p and 13q (containing *RB1*), frequent gains of 3q, 5p, and losses of 17p (containing *TP53*) (Supplementary Fig. 1a). Gains of 3q affected the region containing *SOX2*, recently shown to be focally amplified in squamous-cell lung cancer[19,20]. However, 3q gains in SCLC were less focal than those in squamous-cell lung cancer (Supplementary Fig. 1b). Focal amplifications affected *MYCL1* (5/63 cases) and *MYCN* (4/63 cases)[21,22] (Fig. 1a). A single case harbored a focal amplification of *MYC*. All *MYC* family member amplifications (16% of cases) were mutually exclusive suggesting genetic epistasis[21–23]. Focal amplifications affected 8p12 including *FGFR1* (6% with copy number ≥3.5; Fig. 1b) and 19q12 containing *CCNE1*24. Fluorescent *in-situ* hybridization analyses in 51 independent specimens validated the occurrence of *FGFR1* amplifications in SCLC (n=3, 6%, Fig. 1c). We and others have recently reported focal *FGFR1* amplifications in squamous-cell lung cancer; FGFR inhibitors are currently being tested in such patients[17,19,25]. Thus, *FGFR1*-amplified SCLC might benefit from FGFR inhibition. The only significant focal deletion involved *FHIT*[26] (Fig. 1a, Supplementary Tab. 2).

Mice with conditional deletion of *Rb1* and *p53* develop SCLC[4,27–31] bearing amplifications of *Mycl1*, *Mycn*, and *Nfib*, which were subsequently also found in human SCLC[28]. We analyzed CNAs in 20 SCLC tumors (15 primary tumors and 5 metastases) from *p53/Rb1* conditional knockout mice[4] in order to identify alterations shared by both human and mouse tumors. We found significant amplifications of *Mycl1*, *Mycn*, and of *Nfib* (Fig. 1d). In the 15 primary tumors (Supplementary Fig. 2), *Nfib* did not reach statistical significance, suggesting that *Nfib* amplifications occur later in tumor evolution. While *NFIB* was not significantly amplified in the human tumors, three samples exhibited copy number gain at this locus (data not shown). Furthermore, we identified significant amplifications affecting *E2f2*, a mediator of RB1 function[32] and deletions of the histone acetyl transferase gene *Crebbp* in two mouse tumors (Fig. 1d).

By analyzing transcriptome sequencing data of 15 human tumors we next identified and validated three chimeric transcripts (Fig. 1e, Supplementary Tab. 3). Two contained a fusion partner that was also mutated, *MPRIP-TP53* and *CREBBP-RHBDF1* (Fig. 1e); both of which are predicted to create a loss-of-function of the genes involved (Supplementary Fig. 3a, b). Similarly, we also found a low genomic rearrangement frequency by reconstruction from paired-end whole genome sequencing data of two specimens (Fig. 1f). This low frequency is in accordance with the spectrum of CNAs in these samples exhibiting almost exclusively arm-level events (Supplementary Fig. 4a).

In order to identify possible differences in the overall genomic architecture between surgically resected (i.e., early stage) samples (n=17) and samples obtained by autopsy (i.e.,

late stage, n=10) we compared the spectrum of broad CNAs in these two sets. We computed absolute copy numbers from sequencing data in order to correct for admixture of nontumoral cells and for ploidy (Supplementary Note, Supplementary Fig. 4b), but found no significant difference between resected and autopsy cases (Fig. 2a). Furthermore, there was no difference in the total mutation frequency (Fig. 2b) and no segregation between resected and autopsy cases in an analysis of mutated "*driver*" genes (Fig. 2c, d). We further identified 5 triploid and 2 near-tetraploid cases (n=29) and found no statistical significant overrepresentation of samples with ploidy >2 between resected and autopsy cases (p=0.15). On average we observed a ploidy of 2.3, in line with previously reported studies based on DNA cytometry[5]. Thus, resected early-stage tumors and late-stage tumors are genomically similar, underscoring the representative nature of our analysis.

Compared to global sequencing studies of other tumor types[33–41], SCLC exhibits an extremely high mutation rate of 7.4 protein-changing mutations per million basepairs (Fig. 2b, Supplementary Fig. 5a). This high mutation rate is likely linked to tobacco carcinogens, reflected by an elevated rate of C:G>A:T transversions compared to the neutral mutation rate observed in evolution (Supplementary Fig. 5b)[38,42–44]. In order to identify pathogenetically relevant *driver* genes in the context of frequent background mutations we applied several filters, including analyses of a signature of mutational selection and of gene expression (Fig. 2c, Supplementary Note). In particular, significantly mutated genes showing an expression level lower than 1 FPKM (fractions per kilobase of exon per million fragments mapped) in more than half of the 15 transcriptomes were removed. Using these adjustments only two genes had q-values of ≤ 0.1: *TP53* and *RB1* (Fig. 2d)[22,29,30,45,46]. Remarkably, many of the significant genes were actually not expressed (Supplementary Tab. 4) and none of these mutations were called in the transcriptomes. By contrast, all known tumor suppressors exhibited expression in the upper part of the overall distribution (Supplementary Fig. 6) supporting our strategy for elimination of *passenger* mutations. Additional filters included an analysis of regional clustering of mutations in a given gene (defining a mutational hotspot) and integration with orthogonal datasets and databases (Fig. 2c)[47]. Similar to the analysis of significantly mutated genes, we discarded genes that were enriched for silent mutations. Together, these filters yielded a list of likely *driver* genes in SCLC: *TP53*, *RB1*, *PTEN*, *CREBBP*, *EP300*, *SLIT2*, *MLL, COBL*, and *EPHA7* (Fig. 2d).

SLIT2 showed a pronounced clustering of mutations (5 of 29 cases). The observed mutation spectrum (2 nonsense, 1 frame-shift deletion, 2 missense) (Fig. 3a) together with frequent genomic losses (Supplementary Fig. 7a) suggests that *SLIT2* may be a novel tumor suppressor gene in SCLC. We sequenced *SLIT2* in 26 additional tumors and 34 cell lines and found an overall mutation frequency of 10% (n=89). Slit proteins are secreted ligands for Robo receptors involved in axon guidance and cellular migration[48,49]. Supporting a tumor suppressive function of SLIT2/ROBO1 in the lung, *Robo1* knockout mice fail to develop normal lungs; surviving mice exhibit bronchial hyperplasia[50]. Accordingly, a tumor suppressive role for SLIT2 has recently been implied in lung cancer cell lines[51]. Furthermore, ROBO1 was recently found to be a specific serum biomarker of SCLC[52]. *EPHA7* was recently described as a tumor suppressor gene frequently lost in lymphomas[53]. Given its role in embryonic development and neural tube closure[54], *EPHA7* mutations may contribute to the invasive phenotype of SCLC.

Mutations in *CREBBP* and *EP300* were significantly clustered around the histone acetyltransferase (HAT) domain (Fig. 3b). Of these, mutations affecting the homologous Asp1399 (EP300) and Asp1435 (CREBBP) residues both affect acetylase activity in vitro[55–57]. Furthermore, Gly1411Glu in *CREBBP* has been previously identified in lung cancer[58] and follicular lymphoma[59] and Gly1411Val as well as Asp1435Gly were found in relapsed acute lymphoblastic leukemia[60], suggesting a mutational hotspot. By contrast, the Arg386fs mutation and the *CREBBP–RHBDF1* gene fusion truncate the open reading frame in the amino terminus (Fig. 3c, Supplementary Fig. 3a). Together with the observation of *Crebbp* deletions in mouse SCLC (Fig. 1d) and the recently described *CREBBP–BTBD12* gene fusion in the NCI-H209 SCLC cell line[38], inactivation of *CREBBP* and *EP300* likely plays a major role in SCLC. Focused sequencing of the HAT domain-encoding exons of *CREBBP* and *EP300* in a validation set of 26 additional SCLC tumor specimens and 45 cell lines as well as break-apart FISH performed in 34 SCLC cell lines, confirmed an overall mutation frequency of 18% (point-mutations, indels, and gene rearrangements) (Fig. 3b, c, d). *CREBBP*/*EP300* mutations have recently been described in relapsed acute lymphoblastic leukemia and B-cell lymphoma[57,61] but have not been observed at such high frequency in solid tumors so far. Furthermore, all mutations and most of the deletions of *CREBBP* and *EP300* occurred in mutually exclusive fashion in the total set of 101 samples analyzed suggesting epistasis (Fig. 3e). The observed alterations are predominantly heterozygous supporting haploinsufficiency[57,62]. Thus, even hemizygous deletions occurring in at least 10% of non-mutant samples (Fig. 3e; Supplementary Fig. 7b) may be considered inactivating.

Further supporting the relevance of *CREBBP*/*EP300* mutations in SCLC, all but one (Asn1286Ser in *EP300*) of the missense mutations were classified as being damaging by computational analyses[63]. Furthermore, all HAT domain mutations were located at the interface of substrate binding[56] (Fig. 4a), thus supporting the notion that they may impact catalytic activity. We assessed the functional impact on histone acetylation of the Gly1411Arg, Asp1435Tyr, and Ser1432Pro *CREBBP* mutations (homologous to Gly1375Arg, Asp1399Tyr, and Ser1396Pro in *EP300*) in reconstitution experiments in Crebbp$^{\mathbf{\Delta flox/\Delta flox}}$, Ep300$^{\mathbf{\Delta flox/\Delta flox}}$ (Crebbp/Ep300 Cre-deleted double knockout, or dKO) murine embryonic fibroblasts (MEFs)[64–66]. All three mutations significantly reduced acetylation of histone 3 lysine 18 (H3K18) (Fig. 4b, c). Specifically, Asp1435Tyr induced complete, Gly1411Arg pronounced, and Ser1432Tyr moderate loss of H3K18 acetylation. Furthermore, knockdown of *CREBBP* in the cell line DMS114 that lacks CREBBP HAT domain mutations resulted in a moderate but significant increase of cell proliferation (Fig. 4d, e). Tumors with mutations and hemizygous deletions in *CREBBP*/*EP300* did not exhibit a significantly different pattern of gene expression as compared to wild-type tumors after correcting for multiple hypothesis testing (data not shown), suggesting that global changes in gene expression are not the predominant mechanism by which loss of HAT activity contributes to SCLC pathogenesis. Together, these results support a role for loss of CREBBP/EP300 function in the biology of SCLC.

Another histone-modifying enzyme mutated in SCLC was the methyltransferase gene *MLL*, which was recurrently mutated at isoleucin 960 (Ile960Met)[47]. *MLL* rearrangements occur

in acute leukemia[67,68]. Similarly, recurrent genetic alterations in histone modifying genes appear to be a novel hallmark feature of SCLC.

Confirming previous reports[69], we found mutations in *PTEN* (3 of 29 cases), all of which and are likely (Gly165Glu) or proven (His61Arg, Arg130Gly) to affect phosphatase activity[70], thereby activating the PI3-kinase pathway. We did not observe any mutations in *PIK3CA*[71].

We developed a mathematical model that gives insight into the allelic state of each tumor and yields estimates of tumor heterogeneity (Supplementary Note). On average, we observed a rather low heterogeneity of about 6.5% (Supplemetary Tab. 5). Using the reconstructed allelic states of each tumor, we found that copy-neutral loss of heterozygosity (CNLOH) events (i.e., complete loss of one allele at a given locus combined with a match of the absolute copy number at that locus with the overall ploidy of the sample) were enriched at the *TP53* and *RB1* loci (Fig. 5a, b). Furthermore, all *TP53* and *RB1* mutations in CNLOH regions were early events (Fig. 5b) as their allelic fractions were compatible with the tumor purity. By integrating the different datasets we found that at least one allele of *TP53* and *RB1* was affected by any genomic event (i.e., mutation (including rearrangements), or hemizygous deletion, LOH) in all cases (Fig. 5c). Thus, similar to genetically manipulated mouse models of SCLC, inactivation of *TP53* and *RB1* are early and necessary events in the development of SCLC in humans as well[4,27–31]. Finally, we identified one case, in which the patient had undergone surgery for lung adenocarcinoma three years prior diagnosis of SCLC. While both tumors contained the identical TP53 mutation (Val73fs), the RB1 mutation (Arg251X) was restricted to the SCLC tumor (Supplementary Fig. 8), compatible with trans-differentiation of adenocarcinoma cells to SCLC cells, mediated in part through loss of *RB1*. Acquired resistance of EGFR-mutant lung adenocarcinomas to EGFR inhibition has been linked with trans-differentiation to SCLC[72,73]. It is tempting to speculate that loss of *RB1* may be mechanistically involved in such cases of acquired resistance as well.

Despite methodological challenges (limited sample set, high mutation frequency), integrative genome analyses of human and mouse SCLC afforded sketching a molecular map of this tumor type, condensed in 5 categories (Fig. 5d). The tumor suppressive functions of p53 rely on its acetylation by CREBBP or EP30074-79. However, given the universal loss of p53 function in SCLC, the tumor suppressive functions of CREBBP that we observed are likely independent of p53. One of the best-studied functions of SLIT2 is its involvement in actin polymerization mediated by Cdc4280. We speculate that this property might enhance invasive capabilities and thus contribute to the aggressiveness of SCLC. The reported functions of EPHA753,54 may also contribute to this phenotype. Beyond universal losses of *TP53* and *RB1* and amplifications of *MYCL1*, *MYCN*, *MYC*, we present *PTEN* mutations and *FGFR1* amplifications as potentially therapeutically tractable genome alterations. Finally, we define genomic alterations affecting histone modifying enzymes *CREBBP*, *EP300*, and *MLL* as the second most frequently mutated class of genes in SCLC. In summary, our study represents a significant extension of the current molecular concept of SCLC and, more broadly, provides an example of how integrative computational genome

analyses can provide functionally tractable information in the context of a highly mutated cancer genome.

Supplementary Material

Refer to Web version on PubMed Central for supplementary material.

Authors

Martin Peifer[1,2,*], Lynnette Fernández-Cuesta[1,2,*], Martin L Sos[1,2,3], Julie George[1,2], Danila Seidel[1,2,4], Lawryn H Kasper[5], Dennis Plenker[1,2], Frauke Leenders[1,2,4], Ruping Sun[6], Thomas Zander[1,2,3], Roopika Menon[7], Mirjam Koker[1,2], Ilona Dahmen[1,2], Christian Müller[1,2], Vincenzo Di Cerbo[8], Hans-Ulrich Schildhaus[9], Janine Altmüller[10], Ingelore Baessmann[10], Christian Becker[10], Bram de Wilde[11], Jo Vandesompele[11], Diana Böhm[7], Sascha Ansén[3], Franziska Gabler[2], Ines Wilkening[2], Stefanie Heynck[2], Johannes M Heuckmann[1,2], Xin Lu[1,2], Scott L Carter[12], Kristian Cibulskis[12], Shantanu Banerji[12], Gad Getz[12], Kwon-Sik Park[13,14], Daniel Rauh[15], Christian Grütter[15], Matthias Fischer[16,17], Laura Pasqualucci[18], Gavin Wright[19], Zoe Wainer[19], Prudence Russell[20], Iver Petersen[21], Yuan Chen[21], Erich Stoelben[22], Corinna Ludwig[22], Philipp Schnabel[23], Hans Hoffmann[24], Thomas Muley[24], Michael Brockmann[25], Walburga Engel-Riedel[22], Lucia A Muscarella[26], Vito M Fazio[26], Harry Groen[27], Wim Timens[28], Hannie Sietsma[28], Erik Thunnissen[29], Egbert Smit[30], Daniëlle AM Heideman[29], Peter JF Snijders[29], Federico Cappuzzo[31], Claudia Ligorio[32], Stefania Damiani[32], John Field[33], Steinar Solberg[34], Odd Terje Brustugun[35,36], Marius Lund-Iversen[37], Jörg Sänger[38], Joachim H Clement[39], Alex Soltermann[40], Holger Moch[40], Walter Weder[41], Benjamin Solomon[42], Jean-Charles Soria[43], Pierre Validire[44], Benjamin Besse[43], Elisabeth Brambilla[45,46], Christian Brambilla[45,46], Sylvie Lantuejoul[45,46], Philippe Lorimier[45], Peter M Schneider[47], Michael Hallek[3,4], William Pao[48], Matthew Meyerson[12,49,50,51], Julien Sage[13,14], Jay Shendure[52], Robert Schneider[8,53], Reinhard Büttner[4,9], Jürgen Wolf[3,4], Peter Nürnberg[10,17,54], Sven Perner[7], Lukas C Heukamp[9], Paul K Brindle[5], Stefan Haas[6], and Roman K Thomas[1,2,3,4,9]

Affiliations

[1]Department of Translational Genomics, University of Cologne, Weyertal 115b, 50931 Cologne, Germany [2]Max Planck Institute for Neurological Research with Klaus-Joachim-Zülch Laboratories of the Max Planck Society and the Medical Faculty of the University of Cologne, Gleueler Str. 50, 50931 Cologne, Germany [3]Department I of Internal Medicine and Center of Integrated Oncology Köln-Bonn, University of Cologne, 50924 Cologne, Germany [4]Laboratory of Translational Cancer Genomics, Center of Integrated Oncology Köln – Bonn, University of Cologne, 50924 Cologne, Germany [5]Department of Biochemistry, St Jude Children's Research Hospital, Memphis, Tennessee 38105, USA [6]Max Planck Institute for Molecular Genetics, Ihnestr. 73, 14194 Berlin, Germany [7]Institute of Prostate Cancer Research at the Institute of Pathology, University Hospital of Bonn, Sigmund-Freud-Str. 25, 53127 Bonn, Germany [8]Max Planck Institute of

Immunobiology and Epigenetics, 79108 Freiburg, Germany [9]Department of Pathology, University of Cologne, Kerpener Str. 62, 50937 Cologne, Germany [10]Cologne Center for Genomics, University of Cologne, Cologne, Germany [11]Center for Medical Genetics, Ghent University, De Pintelaan 185, 9000 Ghent, Belgium [12]The Broad Institute of Harvard and MIT, Cambridge, Massachusetts 02142, USA [13]Department of Pediatrics, Stanford University, Stanford, California, USA [14]Department of Genetics, Stanford University, Stanford, California, USA [15]Technical University Dortmund, Department of Chemical Biology, Otto-Hahn-Str. 6, 44227 Dortmund, Germany [16]Department of Pediatric Oncology and Hematology, University Children's Hospital of Cologne, Germany [17]Center for Molecular Medicine Cologne (CMMC), University of Cologne, Cologne, Germany [18]Institute for Cancer Genetics and the Herbert Irving Comprehensive Cancer Center, Columbia University, New York, New York 10032, USA [19]The University of Melbourne Department of Surgery, St Vincent's Hospital, Level 2, Clinical Sciences Building 29 Regent Street, Melbourne, 3065 Victoria, Australia [20]Department of Pathology, St. Vincent's Hospital, Melbourne, 3065 Victoria, Australia [21]Institute of Pathology, Jena University Hospital, Friedrich-Schiller-University, 07743 Jena, Germany [22]Thoracic Surgery, Lungenklinik Merheim, Kliniken der Stadt Köln gGmbH, 51109 Cologne, Germany [23]Institute of Pathology, Im Neuenheimer Feld 220, 69120 Heidelberg, Germany [24]Thoraxklinik-Heidelberg gGmbH, Amalienstr. 5, 69126 Heidelberg, Germany [25]Department of Pathology, Hospital Merheim, Kliniken der Stadt Köln gGmbH, 51109 Cologne, Germany [26]Laboratory of Oncology, IRCCS Casa Sollievo della Sofferenza, Viale Cappuccini, 71013 San Giovanni Rotondo, Italy [27]Department of Pulmonary Diseases, University Medical Centre Groningen, 9713 GZ Groningen, Netherlands [28]Department of Pathology, University Medical Centre Groningen, 9713 GZ Groningen, Netherlands [29]Department of Pathology, VU University Medical Center Amsterdam, 1007 MB Amsterdam, Netherlands [30]Department of Pulmonary Diseases, VU University Medical Center Amsterdam, 1007 MB Amsterdam, Netherlands [31]Department of Medical Oncology, Ospedale Civile, 57100 Livorno, Italy [32]Department of Haematology and Oncologic Science, University Hospital Bologna, 40138 Bologna, Italy [33]Roy Castle Lung Cancer Research Programme, The University of Liverpool Cancer Research Centre, School of Cancer Studies, University of Liverpool Cancer Research Centre, Department of Molecular and Clinical Cancer Medicine, Institute of Translational Medicine, The University of Liverpool. 200 London Road, Liverpool, L3 9TA, UK [34]Department of Thoracic Surgery, Rikshospitalet, Oslo University Hospital, 0027 Oslo, Norway [35]Inst of clinical medicine, Faculty of medicine, University of Oslo, N-0424 Oslo, Norway [36]Dept of oncology, Norwegian Radium Hospital, Oslo University Hospital, N-0310 Oslo, Norway [37]Dept of pathology, Norwegian Radium Hospital, Oslo University Hospital, N-0310 Oslo, Norway [38]Institute for Pathology Bad Berka, 99438 Bad Berka, Germany [39]Department for Internal Medicine II, Jena University Hospital, Friedrich-Schiller University, 07740 Jena, Germany [40]Institute for Surgical Pathology, University Hospital Zurich, 8091 Zurich, Switzerland [41]Division of Thoracic Surgery, University Hospital Zurich, 8091 Zurich, Switzerland

[42]Department of Haematology and Medical Oncology, Peter MacCallum Cancer Centre, Melbourne, 3002 Victoria, Australia [43]Phase I Unit–Department of Medicine, Institute Gustave Roussy, 39 Rue Camille Desmoulins, 94800 Villejuif, France [44]France Service d'Anatomie-Pathologie, Institut Mutualiste Montsouris, 75014 Paris, France [45]Department of Pathology, Université Joseph Fourier, 38041 Grenoble, France [46]Institut Albert Bonniot INSERM U823, Université Joseph Fourier, 38042 Grenoble, France [47]Institute of Legal Medicine, University of Cologne, Melatengürtel 60/62, 50823 Cologne, Germany [48]Vanderbilt-Ingram Cancer Center, Nashville, TN, USA [49]Harvard Medical School, Boston, Massachusetts 02115, USA [50]Department of Medical Oncology, Dana-Farber Cancer Institute, Boston, Massachusetts 02115, USA [51]Center for Cancer Genome Discovery, Dana-Farber Cancer Institute, Boston, Massachusetts 02115, USA [52]University of Washington, Department of Genome Sciences, Foege Building S-250, Box 355065, 3720 15th Ave NE, Seattle, WA 98195-5065, USA [53]Institut de Génétique et de Biologie Moléculaire et Cellulaire, CNRS UMR 7104, INSERM U 964, Université de Strasbourg, 67404 Illkirch, France [54]Cologne Excellence Cluster on Cellular Stress Responses in Aging-Associated Diseases (CECAD), University of Cologne, Cologne, Germany

Acknowledgments

We are indebted to the patients donating their tumor specimens as part of the *Clinical Lung Cancer Genome Project* initiative. Additional biospecimens for this study were obtained from Victorian Cancer Biobank, Melbourne, Australia. The Institutional Review Board (IRB) of each participating institution approved collection and use of all patient specimens in this study. We also thank our colleagues of The Cancer Genome Atlas Research Network (TCGA) and Andrew L. Kung (Dana-Farber Cancer Institute, Children's Hospital, Boston, MA) for invaluable discussion and many helpful comments. This work was supported by the German Ministry of Science and Education (BMBF) as part of the NGFNplus program (grant 01GS08100 to RKT and 01GS08101 to JW and PN), by the Max Planck Society (M.I.F.A.NEUR8061 to RKT), by the Deutsche Forschungsgemeinschaft (DFG) through SFB832 (TP6 to RKT and RTU; TP5 and Z1 to LH and RB) and TH1386/3-1 (to RKT and MLS), by the EU-Framework Programme CURELUNG (HEALTH-F2-2010-258677) (to RKT, JF, EB, CB, SL, BB, and JW), Stand Up To Cancer-American Association for Cancer Research Innovative Research Grant (SU2C-AACR-IR60109) (to RKT and WP), by the Behrens-Weise Foundation (to RKT) and by an anonymous foundation to RKT. MLS is a fellow of the International Association for the Study of Lung Cancer (IASLC). PB and LK thank the St. Jude Cell and Tissue Imaging facility, and support from NIH Cancer Center grant P30 CA021765 and the American Lebanese Syrian Associated Charities of St. Jude Children's Research Hospital. RKT reports the following potential sources of conflict of interest: consulting and lecture fees (Sanofi-Aventis, Merck KGaA, Bayer, Lilly, Roche, Boehringer Ingelheim, Johnson&Johnson, AstraZeneca, Atlas-Biolabs, Daiichi-Sankyo); research support (AstraZeneca, Merck, EOS).

References

1. Gustafsson BI, Kidd M, Chan A, Malfertheiner MV, Modlin IM. Bronchopulmonary neuroendocrine tumors. Cancer. 2008; 113:5–21. [PubMed: 18473355]
2. Travis WD. Lung tumours with neuroendocrine differentiation. European journal of cancer. 2009; 45(Suppl 1):251–66. [PubMed: 19775623]
3. van Meerbeeck JP, Fennell DA, De Ruysscher DK. Small-cell lung cancer. Lancet. 2011; 378:1741–55. [PubMed: 21565397]
4. Park KS, et al. A crucial requirement for Hedgehog signaling in small cell lung cancer. Nature medicine. 2011; 17:1504–8.
5. Travis, WD.; World Health Organization., International Agency for Research on Cancer., International Association for the Study of Lung Cancer & International Academy of Pathology.

Pathology and genetics of tumours of the lung, pleura, thymus and heart. IARC Press, Oxford University Press (distributor); Lyon, Oxford: 2004. p. 344

6. Tiseo M, Ardizzoni A. Current status of second-line treatment and novel therapies for small cell lung cancer. Journal of thoracic oncology: official publication of the International Association for the Study of Lung Cancer. 2007; 2:764–72.
7. Kwak EL, et al. Anaplastic lymphoma kinase inhibition in non-small-cell lung cancer. The New England journal of medicine. 2010; 363:1693–703. [PubMed: 20979469]
8. Lynch TJ, et al. Activating mutations in the epidermal growth factor receptor underlying responsiveness of non-small-cell lung cancer to gefitinib. The New England journal of medicine. 2004; 350:2129–39. [PubMed: 15118073]
9. Paez JG, et al. EGFR mutations in lung cancer: correlation with clinical response to gefitinib therapy. Science. 2004; 304:1497–500. [PubMed: 15118125]
10. Pao W, Chmielecki J. Rational, biologically based treatment of EGFR-mutant non-small-cell lung cancer. Nature reviews– Cancer. 2010; 10:760–74. [PubMed: 20966921]
11. Pao W, et al. EGF receptor gene mutations are common in lung cancers from “never smokers” and are associated with sensitivity of tumors to gefitinib and erlotinib. Proceedings of the National Academy of Sciences of the United States of America. 2004; 101:13306–11. [PubMed: 15329413]
12. Soda M, et al. Identification of the transforming EML4-ALK fusion gene in non-small-cell lung cancer. Nature. 2007; 448:561–6. [PubMed: 17625570]
13. Bergethon K, et al. ROS1 rearrangements define a unique molecular class of lung cancers. Journal of clinical oncology: official journal of the American Society of Clinical Oncology. 2012; 30:863–70. [PubMed: 22215748]
14. Kohno T, et al. KIF5B-RET fusions in lung adenocarcinoma. Nature medicine. 2012; 18:375–7.
15. Lipson D, et al. Identification of new ALK and RET gene fusions from colorectal and lung cancer biopsies. Nature medicine. 2012; 18:382–4.
16. Takeuchi K, et al. RET, ROS1 and ALK fusions in lung cancer. Nature medicine. 2012; 18:378–81.
17. Dutt A, et al. Inhibitor-Sensitive FGFR1 Amplification in Human Non-Small Cell Lung Cancer. PloS one. 2011; 6:e20351. [PubMed: 21666749]
18. Hammerman PS, et al. Mutations in the DDR2 Kinase Gene identify a Novel therapeutic target in squamous cell lung cancer. Cancer Discovery. 2011; 1:78–89. [PubMed: 22328973]
19. Weiss J, et al. Frequent and focal FGFR1 amplification associates with therapeutically tractable FGFR1 dependency in squamous cell lung cancer. Science translational medicine. 2010; 2:62ra93.
20. Bass AJ, et al. SOX2 is an amplified lineage-survival oncogene in lung and esophageal squamous cell carcinomas. Nature genetics. 2009; 41:1238–42. [PubMed: 19801978]
21. Kim YH, et al. Combined microarray analysis of small cell lung cancer reveals altered apoptotic balance and distinct expression signatures of MYC family gene amplification. Oncogene. 2006; 25:130–8. [PubMed: 16116477]
22. Wistuba II, Gazdar AF, Minna JD. Molecular genetics of small cell lung carcinoma. Seminars in oncology. 2001; 28:3–13. [PubMed: 11479891]
23. Gazzeri S, et al. Activation of myc gene family in human lung carcinomas and during heterotransplantation into nude mice. Cancer research. 1991; 51:2566–71. [PubMed: 1850659]
24. Zhao X, et al. Homozygous deletions and chromosome amplifications in human lung carcinomas revealed by single nucleotide polymorphism array analysis. Cancer research. 2005; 65:5561–70. [PubMed: 15994928]
25. Voortman J, et al. Array comparative genomic hybridization-based characterization of genetic alterations in pulmonary neuroendocrine tumors. Proceedings of the National Academy of Sciences of the United States of America. 2010; 107:13040–5. [PubMed: 20615970]
26. Hassan MI, Naiyer A, Ahmad F. Fragile histidine triad protein: structure, function, and its association with tumorogenesis. Journal of cancer research and clinical oncology. 2010; 136:333–50. [PubMed: 20033706]
27. Calbo J, et al. A functional role for tumor cell heterogeneity in a mouse model of small cell lung cancer. Cancer cell. 2011; 19:244–56. [PubMed: 21316603]

28. Dooley AL, et al. Nuclear factor I/B is an oncogene in small cell lung cancer. Genes & development. 2011; 25:1470–5. [PubMed: 21764851]
29. Meuwissen R, et al. Induction of small cell lung cancer by somatic inactivation of both Trp53 and Rb1 in a conditional mouse model. Cancer cell. 2003; 4:181–9. [PubMed: 14522252]
30. Schaffer BE, et al. Loss of p130 accelerates tumor development in a mouse model for human small-cell lung carcinoma. Cancer research. 2010; 70:3877–83. [PubMed: 20406986]
31. Sutherland KD, et al. Cell of origin of small cell lung cancer: inactivation of Trp53 and Rb1 in distinct cell types of adult mouse lung. Cancer cell. 2011; 19:754–64. [PubMed: 21665149]
32. Iaquinta PJ, Lees JA. Life and death decisions by the E2F transcription factors. Current opinion in cell biology. 2007; 19:649–57. [PubMed: 18032011]
33. Berger MF, et al. The genomic complexity of primary human prostate cancer. Nature. 2011; 470:214–20. [PubMed: 21307934]
34. Chapman MA, et al. Initial genome sequencing and analysis of multiple myeloma. Nature. 2011; 471:467–72. [PubMed: 21430775]
35. Ding L, et al. Genome remodelling in a basal-like breast cancer metastasis and xenograft. Nature. 2010; 464:999–1005. [PubMed: 20393555]
36. Jones S, et al. Frequent mutations of chromatin remodeling gene ARID1A in ovarian clear cell carcinoma. Science. 2010; 330:228–31. [PubMed: 20826764]
37. Pleasance ED, et al. A comprehensive catalogue of somatic mutations from a human cancer genome. Nature. 2010; 463:191–6. [PubMed: 20016485]
38. Pleasance ED, et al. A small-cell lung cancer genome with complex signatures of tobacco exposure. Nature. 2010; 463:184–90. [PubMed: 20016488]
39. Puente XS, et al. Whole-genome sequencing identifies recurrent mutations in chronic lymphocytic leukaemia. Nature. 2011; 475:101–5. [PubMed: 21642962]
40. TCGA. Integrated genomic analyses of ovarian carcinoma. Nature. 2011; 474:609–15. [PubMed: 21720365]
41. Varela I, et al. Exome sequencing identifies frequent mutation of the SWI/SNF complex gene PBRM1 in renal carcinoma. Nature. 2011; 469:539–42. [PubMed: 21248752]
42. Karro JE, Peifer M, Hardison RC, Kollmann M, von Grunberg HH. Exponential decay of GC content detected by strand-symmetric substitution rates influences the evolution of isochore structure. Molecular biology and evolution. 2008; 25:362–74. [PubMed: 18042807]
43. Hecht SS. Progress and challenges in selected areas of tobacco carcinogenesis. Chemical research in toxicology. 2008; 21:160–71. [PubMed: 18052103]
44. Rodin SN, Rodin AS. Origins and selection of p53 mutations in lung carcinogenesis. Seminars in cancer biology. 2005; 15:103–12. [PubMed: 15652455]
45. Horowitz JM, et al. Frequent inactivation of the retinoblastoma anti-oncogene is restricted to a subset of human tumor cells. Proceedings of the National Academy of Sciences of the United States of America. 1990; 87:2775–9. [PubMed: 2181449]
46. Mori N, et al. Variable mutations of the RB gene in small-cell lung carcinoma. Oncogene. 1990; 5:1713–7. [PubMed: 2176283]
47. Bamford S, et al. The COSMIC (Catalogue of Somatic Mutations in Cancer) database and website. British journal of cancer. 2004; 91:355–8. [PubMed: 15188009]
48. Wong K, Park HT, Wu JY, Rao Y. Slit proteins: molecular guidance cues for cells ranging from neurons to leukocytes. Current opinion in genetics & development. 2002; 12:583–91. [PubMed: 12200164]
49. Zhou WJ, et al. Slit-Robo signaling induces malignant transformation through Hakai-mediated E-cadherin degradation during colorectal epithelial cell carcinogenesis. Cell research. 2011; 21:609–26. [PubMed: 21283129]
50. Xian J, et al. Inadequate lung development and bronchial hyperplasia in mice with a targeted deletion in the Dutt1/Robo1 gene. Proceedings of the National Academy of Sciences of the United States of America. 2001; 98:15062–6. [PubMed: 11734623]

51. Tseng RC, et al. SLIT2 attenuation during lung cancer progression deregulates beta-catenin and E-cadherin and associates with poor prognosis. Cancer research. 2010; 70:543–51. [PubMed: 20068157]
52. Taguchi A, et al. Lung cancer signatures in plasma based on proteome profiling of mouse tumor models. Cancer cell. 2011; 20:289–99. [PubMed: 21907921]
53. Oricchio E, et al. The Eph-receptor A7 is a soluble tumor suppressor for follicular lymphoma. Cell. 2011; 147:554–64. [PubMed: 22036564]
54. Holmberg J, Clarke DL, Frisen J. Regulation of repulsion versus adhesion by different splice forms of an Eph receptor. Nature. 2000; 408:203–6. [PubMed: 11089974]
55. Muraoka M, et al. p300 gene alterations in colorectal and gastric carcinomas. Oncogene. 1996; 12:1565–9. [PubMed: 8622873]
56. Liu X, et al. The structural basis of protein acetylation by the p300/CBP transcriptional coactivator. Nature. 2008; 451:846–50. [PubMed: 18273021]
57. Pasqualucci L, et al. Inactivating mutations of acetyltransferase genes in B-cell lymphoma. Nature. 2011; 471:189–95. [PubMed: 21390126]
58. Kishimoto M, et al. Mutations and deletions of the CBP gene in human lung cancer. Clinical cancer research: an official journal of the American Association for Cancer Research. 2005; 11:512–9. [PubMed: 15701835]
59. Morin RD, et al. Frequent mutation of histone-modifying genes in non-Hodgkin lymphoma. Nature. 2011; 476:298–303. [PubMed: 21796119]
60. Inthal A, et al. CREBBP HAT domain mutations prevail in relapse cases of high hyperdiploid childhood acute lymphoblastic leukemia. Leukemia: official journal of the Leukemia Society of America, Leukemia Research Fund, U.K. 2012
61. Mullighan CG, et al. CREBBP mutations in relapsed acute lymphoblastic leukaemia. Nature. 2011; 471:235–9. [PubMed: 21390130]
62. Tillinghast GW, et al. Analysis of genetic stability at the EP300 and CREBBP loci in a panel of cancer cell lines. Genes, chromosomes & cancer. 2003; 37:121–31. [PubMed: 12696060]
63. Ng PC, Henikoff S. SIFT: Predicting amino acid changes that affect protein function. Nucleic acids research. 2003; 31:3812–4. [PubMed: 12824425]
64. Kang-Decker N, et al. Loss of CBP causes T cell lymphomagenesis in synergy with p27Kip1 insufficiency. Cancer cell. 2004; 5:177–89. [PubMed: 14998493]
65. Kasper LH, et al. Conditional knockout mice reveal distinct functions for the global transcriptional coactivators CBP and p300 in T-cell development. Molecular and cellular biology. 2006; 26:789–809. [PubMed: 16428436]
66. Kasper LH, et al. CBP/p300 double null cells reveal effect of coactivator level and diversity on CREB transactivation. The EMBO journal. 2010; 29:3660–72. [PubMed: 20859256]
67. Thirman MJ, et al. Rearrangement of the MLL gene in acute lymphoblastic and acute myeloid leukemias with 11q23 chromosomal translocations. The New England journal of medicine. 1993; 329:909–14. [PubMed: 8361504]
68. Yang XJ. The diverse superfamily of lysine acetyltransferases and their roles in leukemia and other diseases. Nucleic acids research. 2004; 32:959–76. [PubMed: 14960713]
69. Yokomizo A, et al. PTEN/MMAC1 mutations identified in small cell, but not in non-small cell lung cancers. Oncogene. 1998; 17:475–9. [PubMed: 9696041]
70. Han SY, et al. Functional evaluation of PTEN missense mutations using in vitro phosphoinositide phosphatase assay. Cancer research. 2000; 60:3147–51. [PubMed: 10866302]
71. Yamamoto H, et al. PIK3CA mutations and copy number gains in human lung cancers. Cancer research. 2008; 68:6913–21. [PubMed: 18757405]
72. Zakowski MF, Ladanyi M, Kris MG. EGFR mutations in small-cell lung cancers in patients who have never smoked. The New England journal of medicine. 2006; 355:213–5. [PubMed: 16837691]
73. Sequist LV, et al. Genotypic and histological evolution of lung cancers acquiring resistance to EGFR inhibitors. Science translational medicine. 2011; 3:75ra26.

74. Gu W, Shi XL, Roeder RG. Synergistic activation of transcription by CBP and p53. Nature. 1997; 387:819–23. [PubMed: 9194564]
75. Brooks CL, Gu W. Ubiquitination, phosphorylation and acetylation: the molecular basis for p53 regulation. Current opinion in cell biology. 2003; 15:164–71. [PubMed: 12648672]
76. Sakaguchi K, et al. DNA damage activates p53 through a phosphorylation-acetylation cascade. Genes & development. 1998; 12:2831–41. [PubMed: 9744860]
77. Kruse JP, Gu W. Modes of p53 regulation. Cell. 2009; 137:609–22. [PubMed: 19450511]
78. Grossman SR, et al. Polyubiquitination of p53 by a ubiquitin ligase activity of p300. Science. 2003; 300:342–4. [PubMed: 12690203]
79. Lill NL, Grossman SR, Ginsberg D, DeCaprio J, Livingston DM. Binding and modulation of p53 by p300/CBP coactivators. Nature. 1997; 387:823–7. [PubMed: 9194565]
80. Wong K, et al. Signal transduction in neuronal migration: roles of GTPase activating proteins and the small GTPase Cdc42 in the Slit-Robo pathway. Cell. 2001; 107:209–21. [PubMed: 11672528]
81. Bordoli L, et al. Functional analysis of the p300 acetyltransferase domain: the PHD finger of p300 but not of CBP is dispensable for enzymatic activity. Nucleic acids research. 2001; 29:4462–71. [PubMed: 11691934]
82. Li H, Ruan J, Durbin R. Mapping short DNA sequencing reads and calling variants using mapping quality scores. Genome research. 2008; 18:1851–8. [PubMed: 18714091]
83. Li H, Durbin R. Fast and accurate short read alignment with Burrows-Wheeler transform. Bioinformatics. 2009; 25:1754–60. [PubMed: 19451168]
84. Ding L, et al. Somatic mutations affect key pathways in lung adenocarcinoma. Nature. 2008; 455:1069–75. [PubMed: 18948947]
85. Scheble VJ, et al. ERG rearrangement is specific to prostate cancer and does not occur in any other common tumor. Modern pathology: an official journal of the United States and Canadian Academy of Pathology, Inc. 2010; 23:1061–7.
86. Laframboise T, Harrington D, Weir BA. PLASQ: a generalized linear model-based procedure to determine allelic dosage in cancer cells from SNP array data. Biostatistics. 2007; 8:323–36. [PubMed: 16787995]
87. Olshen AB, Venkatraman ES, Lucito R, Wigler M. Circular binary segmentation for the analysis of array-based DNA copy number data. Biostatistics. 2004; 5:557–72. [PubMed: 15475419]
88. Sos ML, et al. Predicting drug susceptibility of non-small cell lung cancers based on genetic lesions. The Journal of clinical investigation. 2009; 119:1727–40. [PubMed: 19451690]
89. Querings S, et al. Benchmarking of mutation diagnostics in clinical lung cancer specimens. PloS one. 2011; 6:e19601. [PubMed: 21573178]

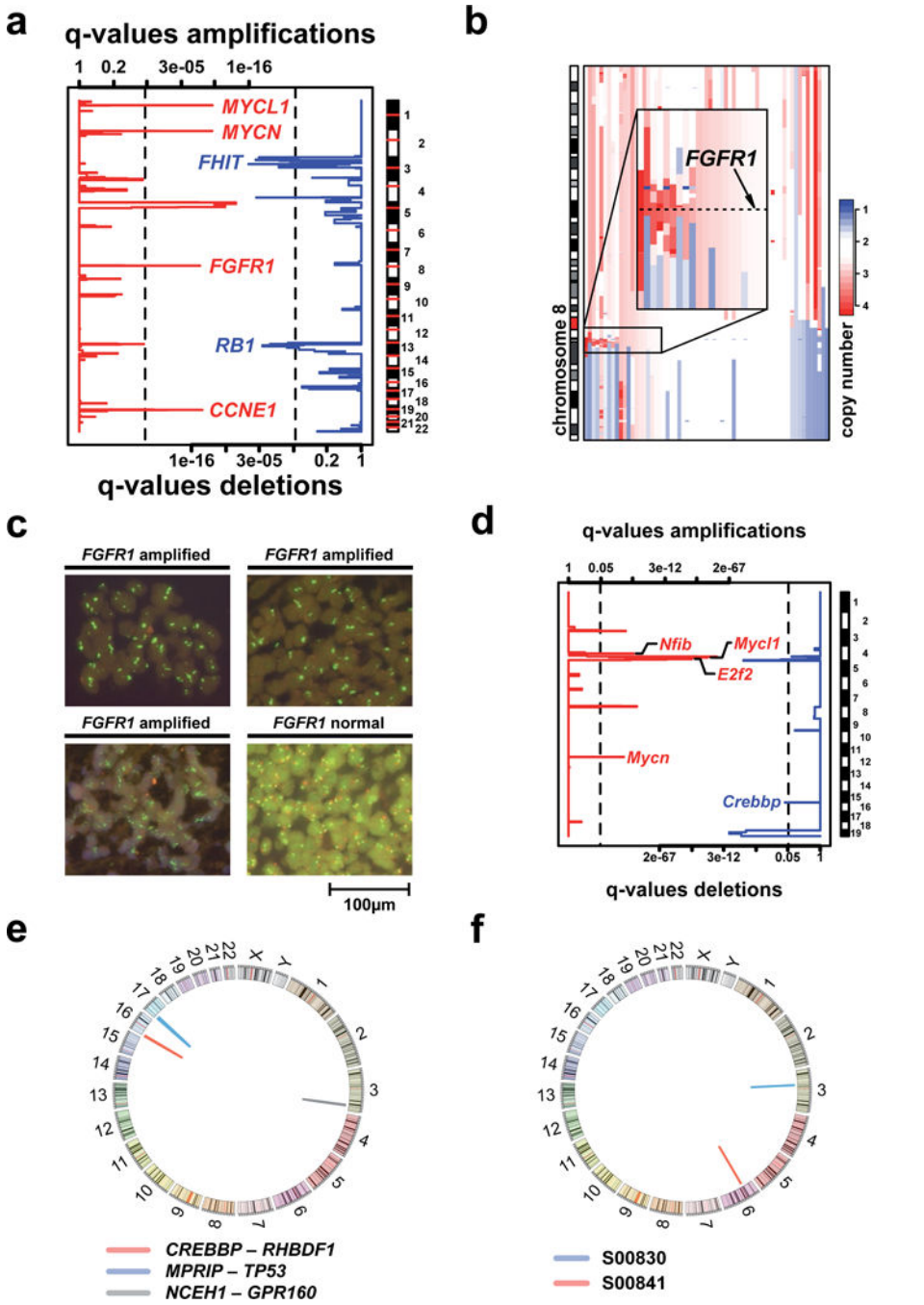

Figure 1.

a) Copy number analysis to detect significantly altered regions across 63 tumors. Statistical significance, expressed by q-values (x-axes), is computed for each genomic location (y-axis) (Supplementary Information). Deletions (blue lines, lower scale) and amplifications (red lines, upper scale) are analyzed independently and vertical dashed black lines indicate the significance threshold of 1%. Focally amplified and deleted regions were identified using narrow thresholds (upper quantile: 10%; lower quantile: 15%) to resolve CNAs down to candidate driver genes. b) CNAs of chromosome 8 containing *FGFR1* (8p12). Samples are

sorted according to the amplitude of *FGFR1* amplification. c) FISH analysis to screen for *FGFR1* amplifications in an independent set of 51 tumors. Quantification of green signals (*FGFR1* specific probe) in comparison to red signals (centromere 8 probe) reveals three *FGFR1* amplified samples. d) Copy number analysis based on array-CGH data of 20 SCLC tumors derived from *p53/Rb1*-deficient mice. Data was analyzed similar to the analysis presented in a). Due to the small sample size, we used a significance threshold of 5% (vertical dashed lines). e) Circos plot of all validated chimeric transcripts detected by transcriptome sequencing. f) Circos plot of validated genomic rearrangements obtained from whole genome sequencing. Both rearrangements affect only portions of the genome smaller than 500kbp. While the structural variant in sample S00841 affects non-coding DNA, the rearrangement in S00830 leads to a loss of exon 7 to 11 of the gene *FOXP1*.

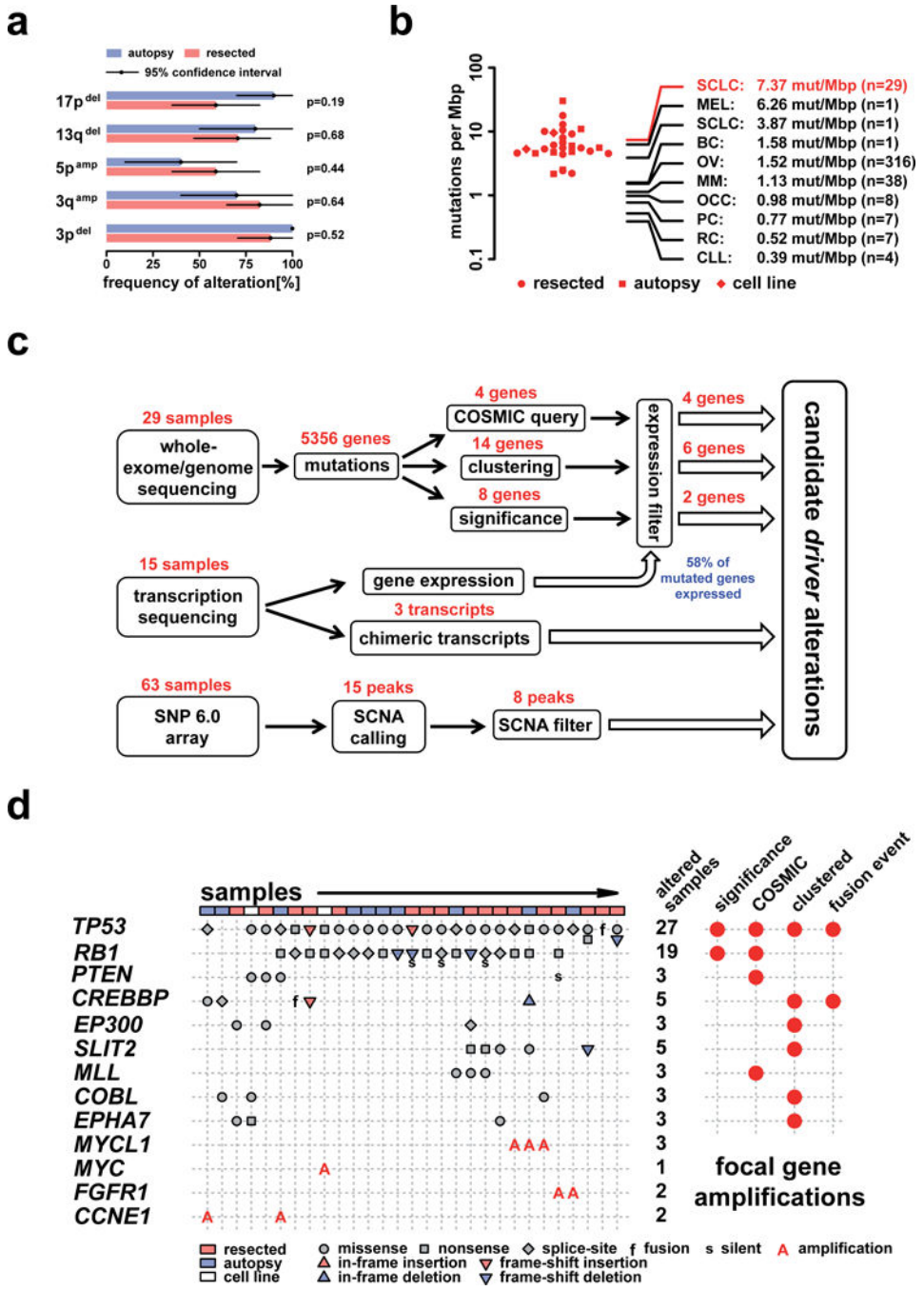

Figure 2.

a) Comparison of broad structural genome alterations between surgically resected and autopsy samples. The analysis is based on absolute copy numbers determined using a reconstruction of the allelic state (Supplementary Note). A broad alteration is assigned to be present if 1/4 of the chromosome arm is altered accordingly. Difference between resected and autopsy samples of broad CNAs in 3p, 3q, 5p, 13q, and 17p were statistically tested by a Fisher's exact test. b) Distribution of the mutation frequency observed in SCLC (points: resected cases; squares: autopsy samples; diamonds: cell lines). The average of the mutation

frequency in SCLC (red lines and label) is compared to various tumor types taken from recent large-scale sequencing studies of: melanoma (MEL)[37], SCLC38, breast cancer (BC)[35], ovarian cancer (OC)[40], multiple myeloma (MM)[34], ovarian clear cell carcinoma (OCC)[36], prostate cancer (PC)[33], renal cell cancer (RC)[41], and chronic lymphocytic leukemia (CLL)[39]. c) A schema showing the various steps of our integrated analysis and filtering procedures. All candidate *driver* genes extracted from sequencing are filtered against gene expression derived from transcription sequencing. CNAs are identified from SNP arrays and candidate CNA regions that are entirely driven by a single SCLC sample were subsequently removed. d) Candidate *driver* genes identified by significance analysis, presence in the COSMIC database, clustered mutations, and genes that are also involved in fusion events. The type of each mutation is shown for every sample including the gene specific total number of mutated samples.

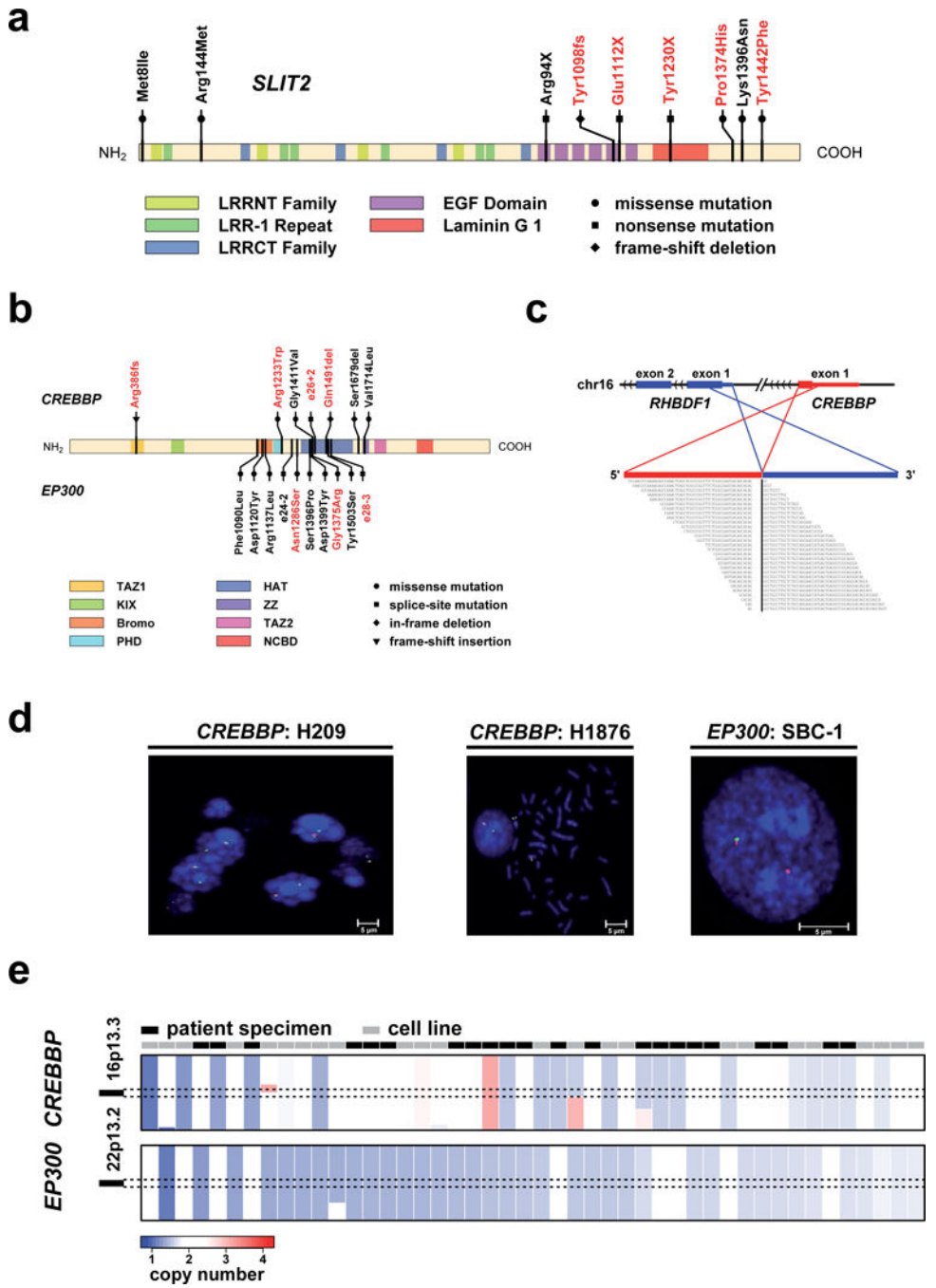

Figure 3.

a) The spectrum of mutations affecting *SLIT2*. Red mutation labels indicate mutations detected by exome sequencing and black labels indicate the results of the extended screen using 454 sequencing. b) Mutations in *CREBBP* and *EP300*. Similar to a), red mutation labels indicate mutations discovered by whole exome sequencing, whereas black mutation labels show the results from the extended sequencing around the HAT domain. c) The structure of the chimeric transcript affecting *RHBDF1* and *CREBPP* is shown. Note, that the genomic scale has been adapted to accommodate exons from both genes (axis break,

dashes). Chimeric reads are shown below. d) Cell lines that show abnormal signals in the break-apart FISH assay of *CREBBP*/*EP300*. In case of *CREBBP*, both cell lines are showing a loss of the telomeric signal (red signal). For *EP300* one cell line also showed a loss of the telomeric signal (here green signal). Break-apart FISH results for *CREBBP* in H209 are shown as a control38. e) Copy number status for *CREBBP* and *EP300* of all samples that show a deletion in one of the two genes (copy numbers ≤ 1.6 are considered as being deleted). Copy numbers are sorted with respect to the minimal copy number between *CREBBP* and *EP300*.

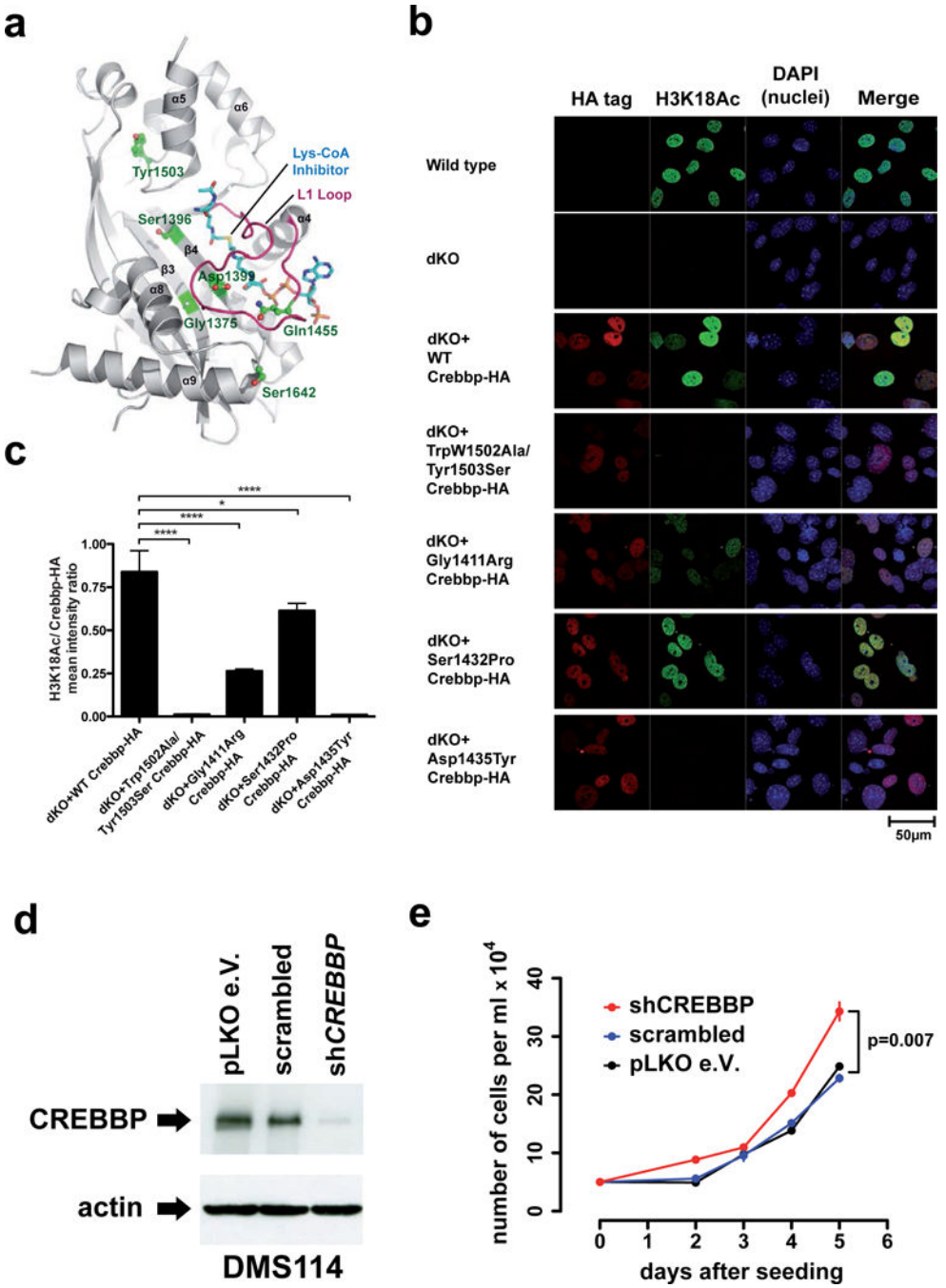

Figure 4.

a) *CREBBP*/*EP300* mutations mapped to the crystal structure of the EP300 HAT domain[56]. All mutations are positioned at the molecular interface involved in Lys-CoA inhibitor binding. In particular, Asp1399 and Gln1455 (equivalent to CREBBP Asp1435 and Gln1491) are located on the substrate-binding loop L1 (red). b) Immunofluorescence was applied to measure levels of acetylated lysine 18 on histone H3 (H3K18Ac) in wild-type MEFs, Crebbp/Ep300 dKO MEFs and dKO MEFs transduced with retroviruses expressing wild-type or SCLC-derived mutants of mouse Crebbp. Human mutations were made at the

equivalent murine amino acid, but human numbering is shown in labels. Crebbp-HA signal, red (CY3); H3K18Ac, green (Alexa 488); nuclei, blue (DAPI). The functionally defective Trp1502Ala/Tyr1503Ser81 was included as a control. c) Quantification of H3K18Ac mean signal intensity per nucleus relative to the HA-tagged Crebbp mean signal intensity. P-values shown are from Bonferroni post test of one way ANOVA. * P<0.05, **** P<0.0001. d) Whole cell lysates of DMS114 cells stably infected with lentiviruses expressing shRNAs targeting *CREBBP* were analyzed for CREBBP protein levels by immunoblotting. e) DMS114 cells stably infected with lentiviral shRNAs targeting *CREBBP* or the indicated control cells were seeded in 6-well plates and counted as triplicates at the indicated time points (*x*-axis). Absolute numbers are given on the *y*-axis and error bars are showing one standard deviation of the mean.

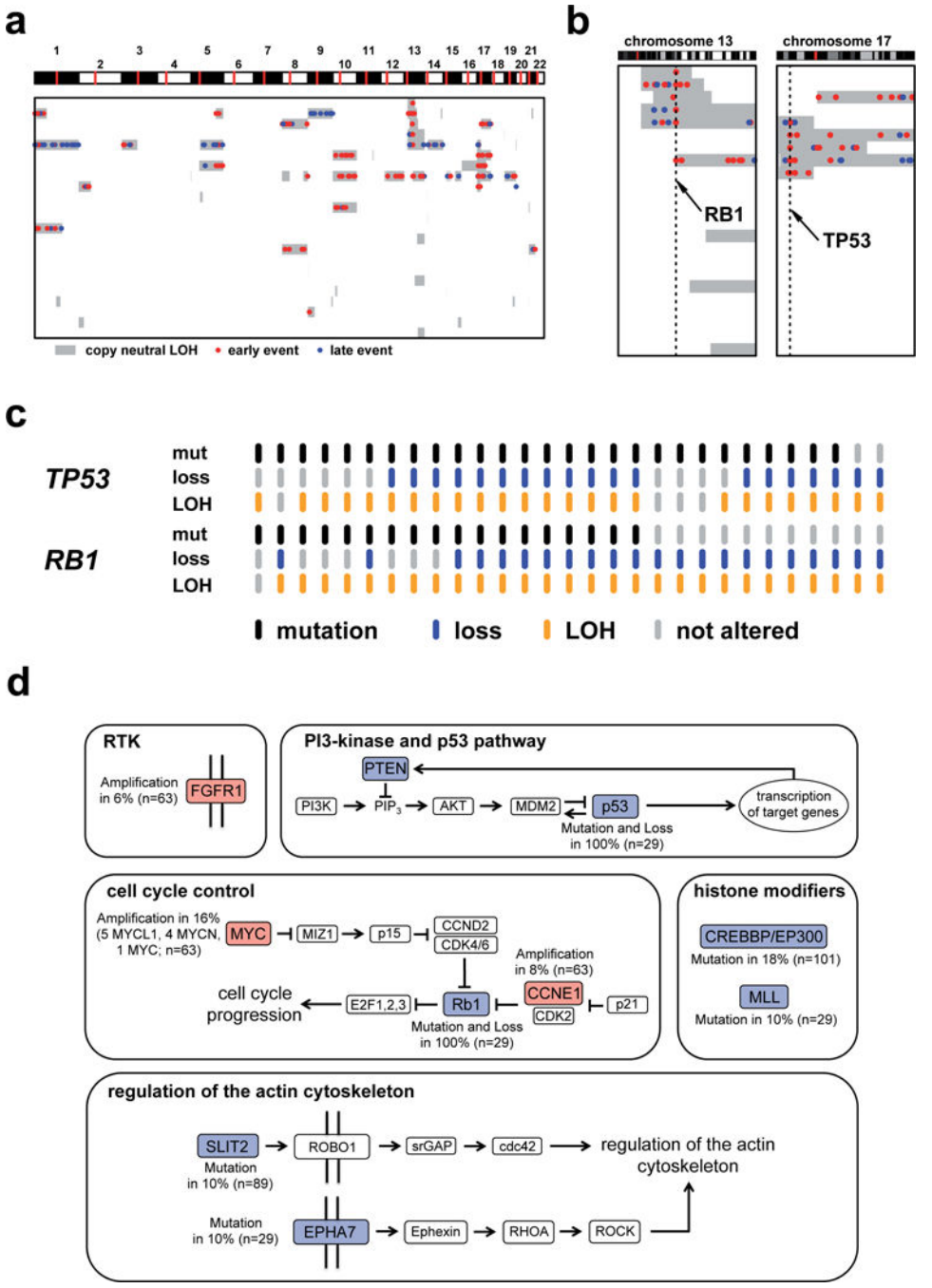

Figure 5.

a) Analysis of copy-neutral LOH events (CNLOH) in SCLC. The allelic state of each exome-sequenced sample was reconstructed by applying a detailed mathematical model (Supplementary Information). Genomic portions that showed a loss of heterozygosity (LOH) and an absolute copy number equal to the overall samples' ploidy are classified CNLOH events. Only samples showing at least one CNLOH event are shown. An analysis of the allelic fraction of somatic mutations in CNLOH regions yields information about the timing of these mutational events. b) *TP53* and *RB1* mutations in CNLOH regions. c) Distribution

of mutations (including rearrangements), hemizygous deletions, and LOH affecting *TP53* and *RB1* across all exome-sequenced samples. d) SCLC driver genes and their mutation frequency mapped to signaling pathways. We classified the occurring mutations into 5 major groups: receptor tyrosine kinase (RTK) alterations, PI3-kinase and p53 pathway, cell cycle control, histone modifiers, and regulation of actin cytoskeleton.